

The Neutrinoless Double Beta Decay in the Colored Zee-Babu Model

Shao-Long Chen^{1,2,*} and Yu-Qi Xiao^{1,†}

¹*Key Laboratory of Quark and Lepton Physics (MoE) and Institute of Particle Physics,
Central China Normal University, Wuhan 430079, China*

²*Center for High Energy Physics, Peking University, Beijing 100871, China*

We study the neutrinoless double beta decay in the colored Zee-Babu model. We consider three cases of the colored Zee-Babu model with a leptoquark and a diquark introduced. The neutrino masses are generated at two-loop level, and the constraints given by tree-level flavor violation processes and muon anomalous magnetic moment $(g-2)_\mu$ have been considered. In our numerical analysis, we find that the standard light neutrino exchange contribution can be canceled by new physics contribution under certain assumption and condition, leading to a hidden neutrinoless double beta decay. The condition can be examined comprehensively by future complementary searches with different isotopes.

I. INTRODUCTION

It is widely assumed that the tiny masses of neutrinos could be generated radiatively where neutrinos are Majorana particles. The Majorana neutrino mass models at two-loop level have been discussed in many previous works, e.g., Ref. [1–8], among which the Zee-Babu model [3, 4] has attracted much attention. The addition of new particles in loops can bring us rich phenomena. However, whether neutrinos are Majorana particles or Dirac particles still remains unknown. The search for the neutrinoless double beta ($0\nu\beta\beta$) decay is the promising way to get us out of this dilemma.

The $0\nu\beta\beta$ decay can be realized if neutrinos are Majorana particles. If one only consider the standard light neutrino exchange, the inverse half-life has the form

$$\left[T_{1/2}^{0\nu\beta\beta}\right]^{-1} = G_\nu |\mathcal{M}_\nu|^2 \frac{|\langle m_{ee} \rangle|^2}{m_e^2}, \quad (1)$$

where G_ν and \mathcal{M}_ν are the phase space factor (PSF) and nuclear matrix element (NME), $\langle m_{ee} \rangle \equiv \sum_i U_{ei}^2 m_i$ is the effective neutrino mass, and m_i ($i = 1, 2, 3$) are the masses of neutrinos. The most stringent limit on the $0\nu\beta\beta$ decay half-life in ^{136}Xe isotope is $T_{1/2}^{0\nu\beta\beta} > 1.07 \times 10^{26}$ yrs given by KamLAND-Zen experiment [9]. They obtained a constraint of $|\langle m_{ee} \rangle| < 61 - 165$ meV. The GERDA experiment has published their result $T_{1/2}^{0\nu\beta\beta} > 1.8 \times 10^{26}$ yrs with isotope ^{76}Ge leading to a similar bound $|\langle m_{ee} \rangle| < 79 - 180$ meV [10]. The future $0\nu\beta\beta$ decay experiments CUPID-1T [11] and LEGEND-1000 [12] using ^{100}Mo and ^{76}Ge isotopes can push the half-life to $10^{27} - 10^{28}$ yrs, leading to a sensitivity to $|\langle m_{ee} \rangle|$ of around 15 meV.

In the effective field theory approach, the $0\nu\beta\beta$ decay can be described in terms of effective low-energy operators [13–18]. The contributions to $0\nu\beta\beta$ decay can be divided into long-range

* E-mail: chensl@mail.ccnu.edu.cn

† E-mail: xiaoyq@mails.ccnu.edu.cn

mechanisms [19–22] and short-range mechanisms [23, 24]. The long-range mechanisms involve light neutrinos exchanged between two point-like vertices, which contain the standard light neutrino exchange. The short-range mechanisms involve the dim-9 effective interaction and are mediated by heavy particles. The decomposition of the short-range operators at tree-level has been completely listed in [25], and at one-loop level has been discussed in [26]. The short-range mechanisms at the LHC have been considered in [27]. An analysis of the standard light neutrino exchange and short-range mechanisms has been given in [28].

In this work, we study three cases of the colored Zee-Babu (cZB) model with a leptoquark and a diquark running in the loops. We consider the realization of tiny neutrino mass and contribution to $0\nu\beta\beta$ decay, with the constraints given by tree-level flavor violation processes and $(g-2)_\mu$ considered. The B physics anomalies and some other phenomena in the cZB model have been explored in [29–36]. The long-range contributions given by the leptoquarks have been considered extensively in the previous discussion [18, 37, 38]. We focus on the short-range impact on neutrinoless double beta decay in this model. The simultaneous introduction of the leptoquarks and diquarks in the cZB model can lead to short-range contribution, which can interfere with the standard light neutrino exchange contribution resulting in cancellation.

We organize our paper as follows. In Sec. II, we show the three cases in the cZB model and briefly review the constraints on them. In Sec. III, we discuss the $0\nu\beta\beta$ decay in each case, including short-range mechanisms and standard light neutrino exchange. Finally, we give our conclusion in Sec. IV.

II. THE MODEL AND CONSTRAINTS

The colored Zee-Babu (cZB) model requires a leptoquark and a diquark to generate the neutrino mass. The diquark is set to be a color sextet under $SU(3)_C \times SU(2)_L \times U(1)_Y$ symmetry where the hypercharge Y is set to be equal to $Q - I_3$. The color triplet is not considered because the coupling of fermions and diquark is antisymmetric, which means the vertex $\bar{d}^c d \omega$ is zero and cannot contribute to the neutrinoless double beta decay process. The cZB model with a leptoquark (LQ) and a color sextet diquark (DQ) has three cases :

- case 1: a singlet LQ $S_1 \sim (\bar{3}, 1, 1/3)$ and a singlet DQ $\omega_1 \sim (6, 1, -2/3)$,
- case 2: a triplet LQ $S_3 \sim (\bar{3}, 3, 1/3)$ and a singlet DQ $\omega_1 \sim (6, 1, -2/3)$,
- case 3: a doublet LQ $\tilde{S}_2 \sim (3, 2, 1/6)$ and a triplet DQ $\omega_3 \sim (6, 3, 1/3)$.

The corresponding quantum numbers of the particles in these cases are summarized in Table I.

In the fermion weak eigenbasis, the Yukawa interactions of these cases can be written as

$$\begin{aligned}
-\mathcal{L}_{Y1} \supset & y_{1SR}^{ij} (\overline{U_R^{i\alpha}})^c E_R^j S_1^{\bar{\alpha}} + y_{1SL}^{ij} (\overline{Q_L^{i\alpha}})^c i\sigma^2 L_L^j S_1^{\bar{\alpha}} + z_{1SR}^{ij} (\overline{U_R^{i\alpha}})^c D_R^{j\beta} S_1^{*\gamma} \epsilon^{\alpha\beta\gamma} \\
& + z_{1SL}^{ij} (\overline{Q_L^{i\alpha}})^c i\sigma^2 Q_L^{j\beta} S_1^{*\gamma} \epsilon^{\alpha\beta\gamma} + z_{1\omega}^{ij} (\overline{D_R^{i\alpha}})^c D_R^{j\beta} \omega_1^{*\bar{\alpha}\bar{\beta}} + \text{h.c.}, \tag{2}
\end{aligned}$$

$$\begin{aligned}
-\mathcal{L}_{Y2} \supset & y_{3S}^{ij} (\overline{Q_L^{i\alpha}})^c i\sigma^2 (\sigma^k S_3^{k\bar{\alpha}}) L_L^j + z_{3S}^{ij} (\overline{Q_L^{i\alpha}})^c i\sigma^2 (\sigma^k S_3^{*k\bar{\beta}})^T Q_L^{j\gamma} \epsilon^{\alpha\beta\gamma} \\
& + z_{1\omega}^{ij} (\overline{D_R^{i\alpha}})^c D_R^{j\beta} \omega_1^{*\bar{\alpha}\bar{\beta}} + \text{h.c.}, \tag{3}
\end{aligned}$$

$$-\mathcal{L}_{Y3} \supset y_{2S}^{ij} (\overline{D_R^{i\alpha}})^T (\tilde{S}_2^\alpha)^T i\sigma^2 L_L^j + z_{3\omega}^{ij} (\overline{Q_L^{i\alpha}})^c i\sigma^2 (\sigma^k \omega_3^{*k\bar{\alpha}\bar{\beta}})^T Q_L^{j\beta} + \text{h.c.}, \tag{4}$$

SM Particles	Quantum Number	New Particles	Quantum Number
$\Phi = (\phi^+, \phi^0)^T$	$(1, 2, 1/2)$	S_1	$(\bar{3}, 1, 1/3)$
$Q_L = (U_L, D_L)^T$	$(3, 2, 1/6)$	\tilde{S}_2	$(3, 2, 1/6)$
$L_L = (\nu_L, E_L)^T$	$(1, 2, -1/2)$	S_3	$(\bar{3}, 3, 1/3)$
U_R	$(3, 1, +2/3)$	ω_1	$(6, 1, -2/3)$
D_R	$(3, 1, -1/3)$	ω_3	$(6, 3, 1/3)$
E_R	$(1, 1, -1)$		

TABLE I. The corresponding quantum numbers of the SM particles and new particles under the gauge symmetry $SU(3)_C \times SU(2)_L \times U(1)_Y$.

where

$$\sigma^k S_3^k = \begin{pmatrix} S_3^{+1/3} & \sqrt{2} S_3^{+4/3} \\ \sqrt{2} S_3^{-2/3} & -S_3^{+1/3} \end{pmatrix}, \quad \sigma^k \omega_3^k = \begin{pmatrix} \omega_3^{+1/3} & \sqrt{2} \omega_3^{+4/3} \\ \sqrt{2} \omega_3^{-2/3} & -\omega_3^{+1/3} \end{pmatrix}, \quad (5)$$

ψ^c is the charge conjugate of ψ , i and j label fermion generations, and (α, β, γ) denote the color of $SU(3)_C$. The σ^k ($k = 1, 2, 3$) are Pauli matrices, S_3^k and ω_3^k are the componets of S_3 and ω_3 under $SU(2)_L$ symmetry, and $\epsilon^{\alpha\beta\gamma}$ is the Levi-Civita symbol. The Yukawa coupling matrices z_{1SL} , $z_{1\omega}$, and $z_{3\omega}$ are symmetric, z_{3S} is antisymmetric, while the other coupling matrices are arbitrary [39]. To study the phenomenologies, we rewrite the Lagrangian in the mass eigenbasis as,

$$\begin{aligned} -\mathcal{L}_{Y1} \supset & y_{1SR}^{ij} \overline{(U_R^{i\alpha})^c} E_R^j S_1^{\bar{\alpha}} + (V^* y_{1SL})^{ij} \overline{(U_L^{i\alpha})^c} E_L^j S_1^{\bar{\alpha}} \\ & - (y_{1SL} U)^{ij} \overline{(D_L^{i\alpha})^c} \nu_L^j S_1^{\bar{\alpha}} + z_{1SR}^{ij} \overline{(U_R^{i\alpha})^c} D_R^{j\beta} S_1^{*\gamma} \epsilon^{\alpha\beta\gamma} \\ & + 2(V^* z_{1SL})^{ij} \overline{(U_L^{i\alpha})^c} D_L^{j\beta} S_1^{*\gamma} \epsilon^{\alpha\beta\gamma} + z_{1\omega}^{ij} \overline{(D_R^{i\alpha})^c} D_R^{j\beta} \omega_1^{*\bar{\alpha}\bar{\beta}} + \text{h.c.}, \end{aligned} \quad (6)$$

$$\begin{aligned} -\mathcal{L}_{Y2} \supset & \sqrt{2}(V^* y_{3S} U)^{ij} \overline{(U_L^{i\alpha})^c} S_3^{-2/3, \bar{\alpha}} \nu_L^j - (y_{3S} U)^{ij} \overline{(D_L^{i\alpha})^c} S_3^{+1/3, \bar{\alpha}} \nu_L^j \\ & - (V^* y_{3S})^{ij} \overline{(U_L^{i\alpha})^c} S_3^{+1/3, \bar{\alpha}} E_L^j - \sqrt{2} y_{3S}^{ij} \overline{(D_L^{i\alpha})^c} S_3^{+4/3, \bar{\alpha}} E_L^j \\ & - 2(z_{3S} V^\dagger)^{ij} \overline{(D_L^{i\alpha})^c} S_3^{-1/3, \beta} U_L^{j\gamma} \epsilon^{\alpha\beta\gamma} + \sqrt{2}(V^* z_{3S} V^\dagger)^{ij} \overline{(U_L^{i\alpha})^c} S_3^{-4/3, \beta} U_L^{j\gamma} \epsilon^{\alpha\beta\gamma} \\ & - \sqrt{2} z_{3S}^{ij} \overline{(D_L^{i\alpha})^c} S_3^{+2/3, \beta} D_L^{j\gamma} \epsilon^{\alpha\beta\gamma} + z_{1\omega}^{ij} \overline{(D_R^{i\alpha})^c} D_R^{j\beta} \omega_1^{*\bar{\alpha}\bar{\beta}} + \text{h.c.}, \end{aligned} \quad (7)$$

$$\begin{aligned} -\mathcal{L}_{Y3} \supset & (y_{2S} U)^{ij} \overline{D_R^{i\alpha}} \tilde{S}_2^{-1/3, \bar{\alpha}} \nu_L^j - y_{2S}^{ij} \overline{D_R^{i\alpha}} \tilde{S}_2^{+2/3, \bar{\alpha}} E_L^j \\ & - 2(z_{3\omega} V^\dagger)^{ij} \overline{(D_L^{i\alpha})^c} \omega_3^{-1/3, \bar{\alpha}\bar{\beta}} U_L^{j\beta} + \sqrt{2}(V^* z_{3\omega} V^\dagger)^{ij} \overline{(U_L^{i\alpha})^c} \omega_3^{-4/3, \bar{\alpha}\bar{\beta}} U_L^{j\beta} \\ & - \sqrt{2} z_{3\omega}^{ij} \overline{(D_L^{i\alpha})^c} \omega_3^{+2/3, \bar{\alpha}\bar{\beta}} D_L^{j\beta} + \text{h.c.} \end{aligned} \quad (8)$$

Here we follow the basis transition $U_L^j \rightarrow (V^\dagger)_{jk} U_L^k$, $D_L^j \rightarrow D_L^j$, $E_L^j \rightarrow E_L^j$ and $\nu_L^j \rightarrow U_{jk} \nu_L^k$ in [40], where V is the Cabibbo-Kobayashi-Maskawa (CKM) matrix, and U is the Pontecorvo-Maki-Nakagawa-Sakata (PMNS) matrix. The scalar potential involving the leptoquark and the diquark fields contains cubic terms

$$V_1 \supset \mu_1 S_1^{\bar{\alpha}} S_1^{\bar{\beta}} \omega_1^{\alpha\beta} + \text{h.c.}, \quad (9)$$

$$\begin{aligned} V_2 \supset & \mu_2 (S_3^{\bar{\alpha}})^T S_3^{\bar{\beta}} \omega_1^{\alpha\beta} + \text{h.c.} \\ = & 2\mu_2 S_3^{-2/3, \bar{\alpha}} S_3^{+4/3, \bar{\beta}} \omega_1^{-2/3, \alpha\beta} + \mu_2 S_3^{+1/3, \bar{\alpha}} S_3^{+1/3, \bar{\beta}} \omega_1^{-2/3, \alpha\beta} + \text{h.c.}, \end{aligned} \quad (10)$$

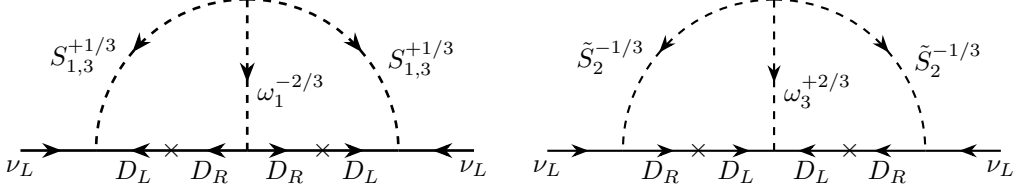


FIG. 1. The two-loop diagrams which generate tiny neutrino masses in the colored Zee-Babu model. The left diagram corresponds to cases 1 and 2, and the right corresponds to case 3.

$$\begin{aligned}
V_3 &\supset \mu_3 (\tilde{S}_2^\alpha)^T (\sigma^k \omega_3^{k,\alpha\beta})^* i \sigma_2 \tilde{S}_2^\beta + \text{h.c.} \\
&= \mu_3 \tilde{S}_2^{+2/3,\alpha} \omega_3^{-1/3,\bar{\alpha}\bar{\beta}} \tilde{S}_2^{-1/3,\beta} + \sqrt{2} \mu_3 \tilde{S}_2^{-1/3,\alpha} \omega_3^{+2/3,\bar{\alpha}\bar{\beta}} \tilde{S}_2^{-1/3,\beta} \\
&\quad - \sqrt{2} \mu_3 \tilde{S}_2^{+2/3,\alpha} \omega_3^{-4/3,\bar{\alpha}\bar{\beta}} \tilde{S}_2^{+2/3,\beta} + \mu_3 \tilde{S}_2^{-1/3,\alpha} \omega_3^{-1/3,\bar{\alpha}\bar{\beta}} \tilde{S}_2^{+2/3,\beta} + \text{h.c.} .
\end{aligned} \tag{11}$$

For simplicity, we assume the quartic couplings of leptoquark and the SM Higgs doublet Φ to be vanishing for case 2 and case 3. In addition, the quartic couplings of ω_3 and Φ are also assumed to be negligible. The leptoquark/diquark multiplets are then degenerate in mass, we denote the masses of S_1, S_2, S_3, ω_1 , and ω_3 as $M_{S_1}, M_{S_2}, M_{S_3}, M_{\omega_1}$, and M_{ω_3} , respectively. In our numerical analysis, the masses of the leptoquarks and diquarks are taken as $M_S \gtrsim 1.5$ TeV and $M_\omega \gtrsim 8$ TeV, which accords with the bounds given by the ATLAS and CMS collaboration [41–47].

A. Neutrino masses

In the colored Zee-Babu model with a leptoquark and a diquark, the neutrino masses can be generated at two-loop level with down-type quarks running in the loop as shown in Fig. 1. The left Feynman diagram corresponds to case 1 and case 2, and the right one to case 3. The neutrino mass matrix elements in flavor basis take the form [29]

$$M_{\nu_a}^{kn} = 24 \mu_a [y_{bS(L)}^T]^{kl} m_{D^l} z_{\omega}^{lm} m_{D^m} y_{bS(L)}^{mn} \mathcal{I}_{lm} \tag{12}$$

$$= 24 \mu [y_{S(L)}^T]^{kl} m_{D^l} z_{\omega}^{lm} m_{D^m} y_{S(L)}^{mn} \mathcal{I}_{lm} , \tag{13}$$

where m_{D^l} is the mass of the l -th generation down-type quark. The superscripts $k, l, m, n = 1, 2, 3$ and the subscripts $a, b, c = 1, 2, 3$ of the couplings are neglected to keep the expression concise. The expression can apply to all three cases. Note that the coupling $y_{S(L)}$ equals y_{1SL} in case 1, y_{3S} in case 2, and y_{2S} in case 3. The \mathcal{I}_{lm} in Eq. (13) is loop integral

$$\mathcal{I}_{lm} = \int \frac{d^4 k}{(2\pi)^4} \int \frac{d^4 q}{(2\pi)^4} \frac{1}{q^2 - m_{D^l}^2} \frac{1}{q^2 - M_S^2} \frac{1}{k^2 - M_S^2} \frac{1}{k^2 - m_{D^m}^2} \frac{1}{(k - q)^2 - M_\omega^2} , \tag{14}$$

where M_S denotes leptoquark S_i mass and M_ω is diquark ω_i mass in different cases. The integral can be simplified as [48]

$$\mathcal{I}_{lm} \simeq \frac{1}{(16\pi^2)^2} \frac{1}{M_S^2} \tilde{I}\left(\frac{M_\omega^2}{M_S^2}\right), \quad \tilde{I}(r) = - \int_0^1 dx \int_0^{1-x} dy \frac{1}{x + (r-1)y + y^2} \ln \frac{y(1-y)}{x + ry} , \tag{15}$$

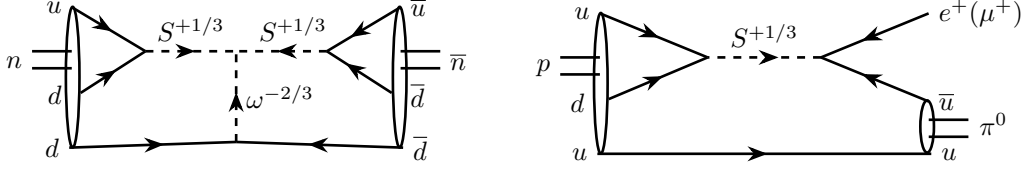


FIG. 2. Feynman diagrams of neutron-antineutron oscillation (left) and proton decay $p \rightarrow \pi^0 e^+ (\mu^+)$ (right) in case 1 and case 2. For case 1, $S^{+1/3} = S_1^{1/3}$ and $\omega^{-2/3} = \omega_1^{-2/3}$. For case 2, $S^{+1/3} = S_3^{+1/3}$ and $\omega^{-2/3} = \omega_3^{-2/3}$.

with the $\tilde{I}(r)$ can be calculated through the numerical integral way. The neutrino mass matrix can be diagonalized by the PMNS matrix U

$$U^T M_\nu U = \hat{M}_\nu = \begin{pmatrix} m_1 & 0 & 0 \\ 0 & m_2 & 0 \\ 0 & 0 & m_3 \end{pmatrix}, \quad (16)$$

where $m_{1,2,3}$ are the masses of active neutrinos $\nu_{1,2,3}$.

B. Neutron-antineutron oscillation and proton decay

With the leptoquark coupling $z_S^{11} \neq 0$ (z_S corresponds to z_{1SR} and $V^* z_{1SL}$ in case 1 and $V^* z_{3S}$ in case 2), case 1 and case 2 can lead to neutron-antineutron oscillation, as shown in Fig. 2. The transition rate of neutron-antineutron oscillation τ^{-1} is proportional to $|(z_S^{11})^2 z_\omega^{11}|$. Using the current limit $\tau \geq 4.7 \times 10^8$ s given by the Super-Kamiokande (Super-K) experiment [49], one can get the bounds

$$|(z_S^{11})^2 z_\omega^{11}| \leq 1.4 \sim 1.7 \times 10^{-16} \times \left[\frac{M_S^4 M_\omega^2}{\mu \cdot \text{TeV}^5} \right]. \quad (17)$$

With $M_S \sim 1.5$ TeV and $M_\omega \sim 8$ TeV, $|(z_S^{11})^2 z_\omega^{11}| \lesssim 10^{-14}$. The construction of operators and detailed calculation of neutron-antineutron oscillation can be found in [50–58]. However, the proton will decay when z_S^{11} and y_S^{11} are both set nonzero. For example, the non-zero couplings can contribute to the process $p \rightarrow \pi^0 e^+ (\mu^+)$ as shown in Fig. 2. With the experimental limit $\tau/B(p \rightarrow \pi^0 e^+) > 2.4 \times 10^{34}$ yrs and $\tau/B(p \rightarrow \pi^0 \mu^+) > 1.6 \times 10^{34}$ yrs given by Super-K [59], there is a strict bound on the couplings with the matrix element inputs from lattice [60, 61]

$$|z_S^{11} y_S^{11}| \lesssim 10^{-26} \times \left[\frac{M_S}{\text{TeV}} \right]^2. \quad (18)$$

where y_S denotes $V^* y_{1SL}$ and y_{1SR} in case 1 and $V^* y_{3S}$ in case 2. One can find that if $M_S \sim 1.5$ TeV and $y_S^{11} \sim 0.01 - 1$, then $z_{S(L/R)}^{11}$ needs to be at $\mathcal{O}(10^{-26} - 10^{-24})$ scale to avoid an inappropriate proton decay, leading to an unobservable neutron-antineutron oscillation. So in the discussion of cases 1 and 2, we assume $z_S = 0$ to escape proton decay.

C. The texture setup and constraints

We show our texture zeros setup of the couplings matrices and list the bounds on the couplings, which are related to $0\nu\beta\beta$ decay in this subsection. The bounds are derived from muon anomalous magnetic moment and tree level flavor violation processes with four-fermion interactions considered.

1. Texture setup

The standard parameterization of the PMNS matrix is

$$U = \begin{pmatrix} 1 & 0 & 0 \\ 0 & c_{23} & s_{23} \\ 0 & -s_{23} & c_{23} \end{pmatrix} \begin{pmatrix} c_{13} & 0 & s_{13}e^{-i\delta} \\ 0 & 1 & 0 \\ -s_{13}e^{i\delta} & 0 & c_{13} \end{pmatrix} \begin{pmatrix} c_{12} & s_{12} & 0 \\ -s_{12} & c_{12} & 0 \\ 0 & 0 & 1 \end{pmatrix} \begin{pmatrix} 1 & 0 & 0 \\ 0 & e^{i\eta_1} & 0 \\ 0 & 0 & e^{i\eta_2} \end{pmatrix}, \quad (19)$$

where $c_{ij}(s_{ij})$ denotes $\cos\theta_{ij}(\sin\theta_{ij})$, δ is the CP phase, and $\eta_{1,2}$ are the extra phases if neutrino are Majorana particles. The best fit values of these neutrino oscillation parameters have been derived in [62–65]. As there are no information about the Majorana phases ranges, they can varies from 0 to 2π freely. To evade constraints from various lepton flavor violation (LFV) processes, we adopt the Yukawa coupling matrices in case 1 as

$$y_{1SL} = V^T \begin{pmatrix} \# & 0 & 0 \\ 0 & 0 & \# \\ \# & \# & \# \end{pmatrix}, \quad y_{1SR} = \begin{pmatrix} \# & 0 & 0 \\ 0 & 0 & 0 \\ 0 & \# & 0 \end{pmatrix}, \quad z_{1\omega} = \begin{pmatrix} \# & 0 & 0 \\ 0 & 0 & \# \\ 0 & \# & \# \end{pmatrix}. \quad (20)$$

The matrix y_{1SL} and $z_{1\omega}$ are set to be complex and y_{1SR} is real. The contribution to neutrinoless double beta decay can survive when couplings $(V^*y_{1SL})^{11} \equiv y_{1SL}^{11}$, y_{1SR}^{11} and $z_{1\omega}^{11}$ (in blue) are set nonzero. Moreover, we have set y_{1SL}^{32} , $y_{1SR}^{32} \neq 0$ (in red) to obtain the muon anomalous magnetic moment $(g-2)_\mu$. The entries of couplings y_{1SL}^{23} , y_{1SR}^{33} , $z_{1\omega}^{33}$, $z_{1\omega}^{23}$ provide enough independent parameters to generate appropriate neutrino mass matrix. It is noted that the first component of the neutrino mass matrix is negligible under these entries with the constraint from the tree-level flavor violation processes $|y_{1SL}^{11}| < 0.12$, as shown in the following subsection, leading to an inconspicuous standard light neutrino exchange $0\nu\beta\beta$ decay. Hence we introduce y_{1SL}^{31} (in teal) to open the standard $0\nu\beta\beta$ decay.

The texture zeros setup of coupling matrices in case 2 and case 3 are similar to those in case 1

$$y_{3S} = V^T \begin{pmatrix} \# & 0 & 0 \\ 0 & 0 & \# \\ \# & \# & \# \end{pmatrix}, \quad z_{1\omega} = \begin{pmatrix} \# & 0 & 0 \\ 0 & 0 & \# \\ 0 & \# & \# \end{pmatrix}, \quad y_{2S} = \begin{pmatrix} \# & 0 & 0 \\ 0 & 0 & \# \\ \# & \# & \# \end{pmatrix}, \quad z_{3\omega} = \begin{pmatrix} \# & 0 & 0 \\ 0 & 0 & \# \\ 0 & \# & \# \end{pmatrix}, \quad (21)$$

with $V^*y_{3S} \equiv y_{2S}'$. Though the coupling $|y_{2S}^{11}|$ could be $\mathcal{O}(1)$ in case 3, we still choose the same form of the matrix to make the analysis consistently.

2. Constraints

The Yukawa couplings are constrained by tree-level flavor violation processes. It is natural to work with effective field theory where the effective Lagrangian can be described with four-fermion interaction operators as the new particles are at TeV scale. The effective Lagrangian involving S_1 leptoquark reads [31]

$$\begin{aligned} \mathcal{L}_{\text{eff},1} = & \frac{1}{2M_{S_1}^2} \left\{ (V^* y_{1SL})^{*ki} (V^* y_{1SL})^{nj} [\overline{E^i} \gamma_\mu P_L E^j] [\overline{U^k} \gamma^\mu P_L U^n] \right. \\ & + y_{1SL}^{*ki} y_{1SL}^{nj} [\overline{\nu^i} \gamma_\mu P_L \nu^j] [\overline{D^k} \gamma^\mu P_L D^n] + y_{1SR}^{*ki} y_{1SR}^{nj} [\overline{E^i} \gamma_\mu P_R E^j] [\overline{U^k} \gamma^\mu P_R U^n] \\ & - \left[y_{1SL}^{*ki} (V^* y_{1SL})^{nj} [\overline{\nu^i} \gamma_\mu P_L E^j] [\overline{D^k} \gamma^\mu P_L U^n] + \text{h.c.} \right] \\ & + \left[y_{1SR}^{*ki} y_{1SL}^{nj} [\overline{\nu^i} P_R E^j] [\overline{D^k} P_R U^n] + \text{h.c.} \right] \\ & + \left[(V^* y_{1SL})^{*ki} y_{1SR}^{nj} [\overline{E^i} P_R E^j] [\overline{U^k} P_R U^n] + \text{h.c.} \right] \\ & - \frac{1}{4} \left[y_{1SR}^{*ki} y_{1SL}^{nj} [\overline{\nu^i} \sigma_{\mu\nu} P_R E^j] [\overline{D^k} \sigma^{\mu\nu} P_R U^n] + \text{h.c.} \right] \\ & \left. - \frac{1}{4} \left[(V^* y_{1SL})^{*ki} y_{1SR}^{nj} [\overline{E^i} \sigma_{\mu\nu} P_R E^j] [\overline{U^k} \sigma^{\mu\nu} P_R U^n] + \text{h.c.} \right] \right\}. \end{aligned} \quad (22)$$

The effective Lagrangians induced by S_3 and \tilde{S}_2 can be written as

$$\begin{aligned} \mathcal{L}_{\text{eff},2} = & \frac{1}{2M_{S_3}^2} \left\{ (V^* y_{3S})^{*ki} (V^* y_{3S})^{nj} [\overline{E^i} \gamma^\mu P_L E^j] [\overline{U^k} \gamma_\mu P_L U^n] \right. \\ & + 2(V^* y_{3S})^{*ki} (V^* y_{3S})^{nj} [\overline{\nu^i} \gamma^\mu P_L \nu^j] [\overline{U^k} \gamma_\mu P_L U^n] \\ & + 2y_{3S}^{*ki} y_{3S}^{nj} [\overline{E^i} \gamma^\mu P_L E^j] [\overline{D^k} \gamma_\mu P_L D^n] \\ & + y_{3S}^{*ki} y_{3S}^{nj} [\overline{\nu^i} \gamma^\mu P_L \nu^j] [\overline{D^k} \gamma_\mu P_L D^n] \\ & \left. + \left[y_{3S}^{*ki} (V^* y_{3S})^{nj} [\overline{\nu^i} \gamma_\mu P_L E^j] [\overline{D^k} \gamma_\mu P_L U^n] + \text{h.c.} \right] \right\}, \end{aligned} \quad (23)$$

$$\mathcal{L}_{\text{eff},3} = -\frac{y_{2S}^{*ki} y_{2S}^{nj}}{2M_{\tilde{S}_2}^2} \left\{ [\overline{E^i} \gamma^\mu P_L E^j] [\overline{D^k} \gamma_\mu P_R D^n] + [\overline{\nu^i} \gamma^\mu P_L \nu^j] [\overline{D^k} \gamma_\mu P_R D^n] \right\}. \quad (24)$$

The constraints on the Wilson coefficient ϵ^{ijkn} have been derived in [66–69], where

$$|\epsilon^{ijkn}| = \text{Const.} \times \frac{|y_{S(L)}^{(r)ki} y_{S(L)}^{(r)nj}|}{4\sqrt{2}G_F M_S^2}, \quad (25)$$

with the constant equals 1 in case 1 and case 3 while the constant takes as 1 or 2 in the case 2. Here we have taken the bounds from [69] and have listed some of them in Table II which are related to the couplings that can contribute to neutrinoless double beta decay process. However, one needs to pay attention that bounds on the couplings $|y_{S(L)}^{*ki} y_{S(L)}^{nj}|$ can be derived from the numerical combined calculation of the bounds on $|y_{S(L)}^{ki} y_{S(L)}^{nj}|$ and $|y_{S(L)}^{*ki} y_{S(L)}^{nj}|$ in case 1 and case 2. Moreover, the neutral meson mixing can be contributed by the diquarks. The $B_d^0 - \bar{B}_d^0$ mixing needs to be concerned under our texture setup. The 95% allowed range of the couplings [70] is

$$|z_{1(3)\omega}^{11} z_{1(3)\omega}^{33}| < 4.6(2.3) \times 10^{-5} \times \left(\frac{M_{\omega 1(3)}}{\text{TeV}} \right)^2. \quad (26)$$

Coefficients	Constraints	Coefficients	Constraints	Coefficients	Constraints
$ y'_{1SL}{}^{11}y_{1SL}{}^{11} $	6.88×10^{-3}	$ y'_{1SL}{}^{11}y_{1SL}{}^{31} $	1.61×10^{-2}	$ y'_{1SL}{}^{11}y_{1SL}{}^{32} $	2.57×10^{-1}
$ y'_{1SL}{}^{11}y_{1SL}{}^{23} $	3.10×10^{-4}	$ y'_{1SL}{}^{11}y_{1SL}{}^{33} $	2.41×10^{-1}	$ y'_{1SR}{}^{11}y_{1SR}{}^{11} $	6.5×10^{-1}
$ y'_{1SR}{}^{11}y_{1SL}{}^{32} $	5.87	$ y'_{1SR}{}^{11}y_{1SL}{}^{23} $	5.87	$ y'_{1SR}{}^{11}y_{1SL}{}^{33} $	10.2
$ y'_{3S}{}^{11}y_{3S}{}^{11} $	6.78×10^{-3}	$ y'_{3S}{}^{11}y_{3S}{}^{31} $	4.02×10^{-3}	$ y'_{3S}{}^{11}y_{3S}{}^{32} $	4.66×10^{-4}
$ y'_{3S}{}^{11}y_{3S}{}^{23} $	3.10×10^{-4}	$ y'_{3S}{}^{11}y_{3S}{}^{33} $	1.38×10^{-1}		
$ y'_{2S}{}^{11}y_{2S}{}^{11} $	1.78	$ y'_{2S}{}^{11}y_{2S}{}^{31} $	1.32×10^{-2}	$ y'_{2S}{}^{11}y_{2S}{}^{32} $	1.32×10^{-2}
$ y'_{2S}{}^{11}y_{2S}{}^{23} $	3.23×10^{-1}	$ y'_{2S}{}^{11}y_{2S}{}^{33} $	2.71×10^{-1}		

TABLE II. The constraints on the couplings of the leptoquarks, $y'_{1SL}, y'_{1SR}, y'_{3SL}, y'_{2S}$, which can contribute to $0\nu\beta\beta$ decay. The bounds are taken from [69] with the unit of $(M_S/\text{TeV})^2$.

The muon anomalous magnetic moments $a_\mu = (g - 2)_\mu/2$ can also give information on the couplings. The latest result of muon anomalous magnetic moment has been presented by Muon $g - 2$ collaboration [71] as

$$\Delta a_\mu \equiv a_\mu^{\text{exp}} - a_\mu^{\text{SM}} = (2.51 \pm 0.59) \times 10^{-9}, \quad (27)$$

which has a 4.2σ discrepancy. The expression of muon anomalous magnetic moment in case 1 can be simplified as [72]

$$\Delta a_\mu(S_1) \simeq \frac{3m_\mu^2}{8\pi^2 M_{S_1}^2} \frac{m_t}{m_\mu} \text{Re}[y'_{1SR}{}^{32}y_{1SL}^{*32}] \left[\frac{1}{3}f_1\left(\frac{m_t^2}{m_{S_1}^2}\right) + \frac{2}{3}f_2\left(\frac{m_t^2}{m_{S_1}^2}\right) \right]. \quad (28)$$

While for case 2 and 3, the contributions are

$$\begin{aligned} \Delta a_\mu(S_3) &\simeq \frac{3m_\mu^2}{8\pi^2 M_{S_3}^2} \sum_q |y'_{3S}{}^{q2}|^2 \left[\frac{1}{3}f_3\left(\frac{m_q^2}{m_{S_3}^2}\right) + \frac{2}{3}f_4\left(\frac{m_q^2}{m_{S_3}^2}\right) \right], \\ \Delta a_\mu(\tilde{S}_2) &\simeq \frac{3m_\mu^2}{8\pi^2 M_{\tilde{S}_2}^2} \sum_q |y'_{2S}{}^{q2}|^2 \left[\frac{2}{3}f_3\left(\frac{m_q^2}{m_{\tilde{S}_2}^2}\right) + \frac{1}{3}f_4\left(\frac{m_q^2}{m_{\tilde{S}_2}^2}\right) \right], \end{aligned} \quad (29)$$

with the functions f_i are defined in [72]. To explain the discrepancy, the couplings in case 1 have the relation $\text{Re}[y'_{1SR}{}^{32}y_{1SL}^{*32}] \sim 8.48 \times 10^{-2}$ with the leptoquark mass $M_{S_1} = 1.5$ TeV. However, in case 2 and case 3, the contribution to muon anomalous magnetic moment Δa_μ are negligible since there is no chiral-enhancement m_q/m_μ for these two cases.

After taking accounting of all the constraints mentioned, the parameter regions taken in our numerical analysis are

$$\begin{aligned} \text{case 1 : } &|y'_{1SL}{}^{11}| < 0.12, |y'_{1SL}{}^{31,32}| < 0.3, |y'_{1SL}{}^{33}| < 0.4, |y'_{1SL}{}^{23}| < 0.005, \\ &|y'_{1SR}{}^{11}| < 1.2, \text{Re}[y'_{1SR}{}^{32}y_{1SL}^{*32}] \sim 0.0848, |z_{1\omega}^{11}| < 1.5, |z_{1\omega}^{33}| < 0.001, \end{aligned} \quad (30)$$

$$\begin{aligned} \text{case 2 : } &|y'_{3S}{}^{11}| < 0.12, |y'_{3S}{}^{31}| < 0.07, |y'_{3S}{}^{32}| < 0.008, |y'_{3S}{}^{33}| < 0.4, \\ &|y'_{3S}{}^{23}| < 0.005, |z_{1\omega}^{11}| < 1.5, |z_{1\omega}^{33}| < 0.002, \end{aligned} \quad (31)$$

$$\begin{aligned} \text{case 3 : } &|y'_{2S}{}^{11}| < 1.5, |y'_{2S}{}^{31}| < 0.01, |y'_{2S}{}^{32}| < 0.01, |y'_{2S}{}^{33}| < 0.3, \\ &|y'_{2S}{}^{23}| < 0.3, |z_{3\omega}^{11}| < 0.01, |z_{3\omega}^{33}| < 0.15, \end{aligned} \quad (32)$$

and the $z_{i\omega}^{23}(i = 1, 3)$ in each case are set to be $|z_{i\omega}^{23}| < 1.5$. We take $\mu = M_S = 1.5$ TeV and $M_\omega = 8$ TeV in our following discussion.

III. THE NEUTRINOLESS DOUBLE BETA DECAY

The $0\nu\beta\beta$ decay can be divided into short-range and long-range mechanisms. To study how short-range contributions impact the $0\nu\beta\beta$ decay in the cZB model, we briefly review the general formula of the short-range mechanisms via the effective field theory approach and give numerical analysis in this section.

A. The short-range $0\nu\beta\beta$ decay

The short-range $0\nu\beta\beta$ decay operator can be written as $\mathcal{O}^{0\nu\beta\beta} \propto \bar{u}ud\bar{e}e$, a dim-9 operator. The scalar mediated tree-level topologies and the decomposition of this operator has been listed in [25]. We follow the general parameterization of effective short-range Lagrangian in [23, 28]

$$\begin{aligned} \mathcal{L}_{SR} = \frac{G_F^2 V_{ud}^2}{2m_p} \sum_{X,Y,Z} \left(\epsilon_1^X J_X J_Y j_Z + \epsilon_2^X J_X^{\mu\nu} J_{Y,\mu\nu} j_Z + \epsilon_3^X J_X^\mu J_{Y,\mu} j_Z \right. \\ \left. + \epsilon_4^X J_X^\mu J_{Y,\mu\nu} j^\nu + \epsilon_5^X J_X^\mu J_Y j_\mu \right) + \text{h.c.} \end{aligned} \quad (33)$$

$$= \frac{G_F^2 V_{ud}^2}{2m_p} \sum_{X,i} \epsilon_i^X \mathcal{O}_{i,X}^{0\nu\beta\beta} + \text{h.c.}, \quad (34)$$

where G_F is the Fermi constant, m_p is the proton mass, V_{ud} is the ud component of the CKM matrix, and the dimensionless effective couplings are defined as $\epsilon_i^X = \epsilon_i^{XYZ}$ ($X, Y, Z = R/L$). The J and j , respectively, denote the quark and electron currents as

$$\begin{aligned} J_{R/L} = \bar{u}(1 \pm \gamma_5)d, \quad J_{R,L}^\mu = \bar{u}\gamma^\mu(1 \pm \gamma_5)d, \quad J_{R/L}^{\mu\nu} = \bar{u}\sigma^{\mu\nu}(1 \pm \gamma_5)d, \\ j_{R/L} = \bar{e}(1 \mp \gamma_5)e^c, \quad j^\mu = \bar{e}\gamma^\mu\gamma_5 e^c. \end{aligned} \quad (35)$$

One can express the effective operators in terms of the quark and electron currents as [24, 25]

$$\begin{aligned} \mathcal{O}_{1,XYZ}^{0\nu\beta\beta} \equiv J_X J_Y j_Z, \quad \mathcal{O}_{2,XYZ}^{0\nu\beta\beta} \equiv J_X^{\mu\nu} J_{Y,\mu\nu} j_Z, \quad \mathcal{O}_{3,XYZ}^{0\nu\beta\beta} \equiv J_X^\mu J_{Y,\mu} j_Z, \\ \mathcal{O}_{4,XY}^{0\nu\beta\beta} \equiv J_X^\mu J_{Y,\mu\nu} j^\nu, \quad \mathcal{O}_{5,XY}^{0\nu\beta\beta} \equiv J_X^\mu J_Y j_\mu. \end{aligned} \quad (36)$$

The following expression gives $0\nu\beta\beta$ decay inverse half-life involving the short-range mechanism and light-neutrino exchange [28]

$$\begin{aligned} \left[T_{1/2}^{0\nu\beta\beta} \right]^{-1} = G_{11+}^{(0)} \left| \sum_{i=1}^3 \epsilon_i^{XYL} \mathcal{M}_i^{XY} + \epsilon_\nu \mathcal{M}_\nu \right|^2 + G_{11+}^{(0)} \left| \sum_{i=1}^3 \epsilon_i^{XYR} \mathcal{M}_i^{XY} \right|^2 + G_{66}^{(0)} \left| \sum_{i=4}^5 \epsilon_i^{XY} \mathcal{M}_i^{XY} \right|^2 \\ + G_{16}^{(0)} \times 2\text{Re} \left[\left(\sum_{i=1}^3 \epsilon_i^{XYL} \mathcal{M}_i^{XY} - \sum_{i=1}^3 \epsilon_i^{XYR} \mathcal{M}_i^{XY} + \epsilon_\nu \mathcal{M}_\nu \right) \left(\sum_{i=4}^5 \epsilon_i^{XY} \mathcal{M}_i^{XY} \right)^* \right] \\ + G_{11-}^{(0)} \times 2\text{Re} \left[\left(\sum_{i=1}^3 \epsilon_i^{XYL} \mathcal{M}_i^{XY} + \epsilon_\nu \mathcal{M}_\nu \right) \left(\sum_{i=1}^3 \epsilon_i^{XYR} \mathcal{M}_i^{XY} \right)^* \right], \end{aligned} \quad (37)$$

where ϵ_i^X are the effective couplings shown in Eq. (34), \mathcal{M}_i^{XY} are the NMEs with the short-range mechanism and \mathcal{M}_ν is the NMEs with the light neutrino exchange. The dimensionless parameters

Isotope	$T_{1/2}^{0\nu}$ [10 ²⁵ yrs]	$G_{11+}^{(0)}$	$G_{11-}^{(0)}$	$G_{16}^{(0)}$	$G_{66}^{(0)}$
⁷⁶ Ge	18 [10]	2.360	-0.280	0.870	1.320
⁸² Se	0.24 [74]	10.19	-0.712	2.925	5.450
¹⁰⁰ Mo	0.15 [75]	15.91	-1.053	4.456	8.482
¹²⁸ Te	0.011 [76]	0.585	-0.156	0.313	0.371
¹³⁰ Te	2.2 [77]	14.20	-1.142	4.367	7.672
¹³⁶ Xe	10.7 [9]	14.56	-1.197	4.524	7.876

TABLE III. The lower limits for the decay half-life time of different isotopes from different experiments and the numerical values of the phase space factors (PSFs) in units of 10⁻¹⁵ yr⁻¹ [28].

Isotope	\mathcal{M}_1^{XX}	\mathcal{M}_2^{XX}	\mathcal{M}_3^{XX}	\mathcal{M}_4^{XX}	\mathcal{M}_5^{XX}	\mathcal{M}_ν
⁷⁶ Ge	5300	-174	-200	-158	202	-6.64
⁸² Se	4030	-144	-171	-134	114	-5.46
¹⁰⁰ Mo	12400	-189	-124	-134	1230	-5.27
¹²⁸ Te	4410	-134	-154	-130	205	-4.80
¹³⁰ Te	4030	-122	-141	-109	187	-4.40
¹³⁶ Xe	3210	-96.1	-111	-86.0	147	-3.60

TABLE IV. The numerical values of the NMEs for short-range operators and light-neutrino exchange. The values are calculated within the microscopic interacting boson model and axial coupling quenched $g_A = 1.0$ [28].

ϵ_ν can be written as $\epsilon_\nu = \langle m_{ee} \rangle / m_e$, where $\langle m_{ee} \rangle \equiv \sum_i U_{ei}^2 m_i$ is the effective Majorana neutrino mass and m_e is the electron mass. The $G_{11+}^{(0)}$, $G_{11-}^{(0)}$, $G_{16}^{(0)}$, and $G_{66}^{(0)}$ are the phase space factors (PSFs) defined in [73]. The PSFs numerical values of different isotopes are taken from [28], as shown in Table III. The first column is the lower limits for the decay half-life of different isotopes [9, 10, 74–77]. The Table IV shows the values of light neutrino exchange NME \mathcal{M}_ν and short-range mechanism NMEs \mathcal{M}_i^{XY} within the microscopic interacting boson model [28]. We just list the values of \mathcal{M}_i^{XX} since both of the quark currents in the cZB models are right-handed, i.e., $X = Y = R$.

The effective operators in the three cases can be written as

$$\begin{aligned}
\text{case 1 : } & (\overline{u_L e_L})(\overline{u_L e_L})(d_R d_R) \rightarrow \frac{1}{48} \mathcal{O}_1^{RRL} - \frac{1}{192} \mathcal{O}_2^{RRL}, \\
& (\overline{u_L e_L})(\overline{u_R e_R})(d_R d_R) \rightarrow \frac{1}{96i} \mathcal{O}_4^{RR} - \frac{1}{48} \mathcal{O}_5^{RR}, \\
& (\overline{u_R e_R})(\overline{u_R e_R})(d_R d_R) \rightarrow -\frac{1}{48} \mathcal{O}_3^{RRR}, \tag{38}
\end{aligned}$$

$$\text{case 2 : } (\overline{u_L e_L})(\overline{u_L e_L})(d_R d_R) \rightarrow \frac{1}{48} \mathcal{O}_1^{RRL} - \frac{1}{192} \mathcal{O}_2^{RRL}, \tag{39}$$

$$\text{case 3 : } (\overline{u_L u_L})(d_R \overline{e_L})(d_R \overline{e_L}) \rightarrow \frac{1}{48} \mathcal{O}_1^{RRL} - \frac{1}{192} \mathcal{O}_2^{RRL}. \tag{40}$$

The corresponding Feynman diagrams in different cases are shown in Fig. 3. The effective couplings ϵ_i^χ in different cases are

$$\text{case 1 : } \epsilon_1^{RRL} = +\frac{1}{48} \frac{2m_p}{G_F^2 V_{ud}^2} \frac{4(y_{1SL}^{*11})^2 z_{1\omega}^{11} \mu_1}{M_{S_1}^4 M_{\omega_1}^2}, \quad \epsilon_2^{RRL} = -\frac{1}{4} \epsilon_1^{RRL},$$

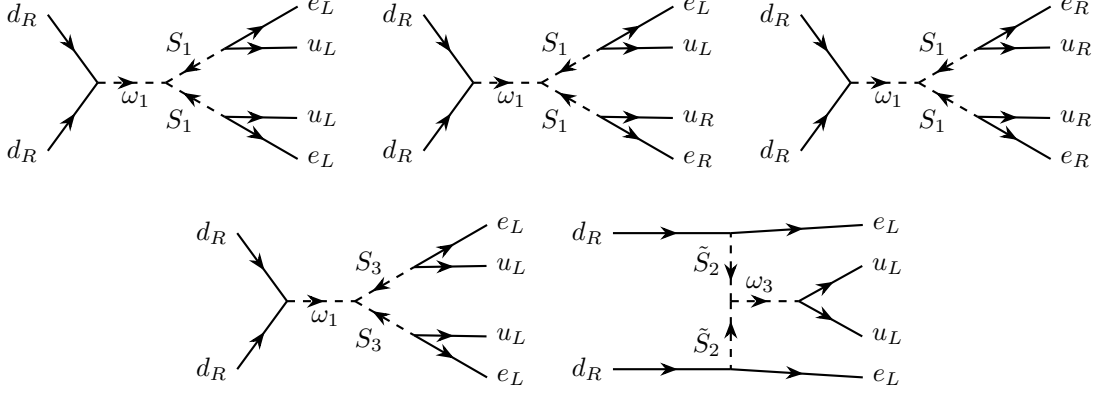


FIG. 3. The Feynman diagrams of neutrinoless double beta decay in the colored Zee-Babu model. The first row corresponds to case 1. The two diagrams in the second row coorespond to case 2 (left) and case 3 (right).

$$\begin{aligned} \epsilon_3^{RRR} &= -\frac{1}{48} \frac{2m_p}{G_F^2 V_{ud}^2} \frac{4(y_{1SR}^{*11})^2 z_{1\omega}^{11} \mu_1}{M_{S_1}^4 M_{\omega_1}^2}, \\ \epsilon_4^{RR} &= +\frac{1}{96i} \frac{2m_p}{G_F^2 V_{ud}^2} \frac{4y_{1SR}^{*11} y_{1SL}'^{*11} z_{1\omega}^{11} \mu_1}{M_{S_1}^4 M_{\omega_1}^2}, \quad \epsilon_5^{RR} = -2i\epsilon_4^{RR}, \end{aligned} \quad (41)$$

$$\text{case 2 : } \epsilon_1^{RRL} = +\frac{1}{48} \frac{2m_p}{G_F^2 V_{ud}^2} \frac{4(y_{3S}^{*11})^2 z_{1\omega}^{11} \mu_2}{M_{S_3}^4 M_{\omega_1}^2}, \quad \epsilon_2^{RRL} = -\frac{1}{4}\epsilon_1^{RRL}, \quad (42)$$

$$\text{case 3 : } \epsilon_1^{RRL} = -\frac{1}{48} \frac{2m_p}{G_F^2 V_{ud}^2} \frac{4(y_{2S}^{*11})^2 (V^* z_{3\omega} V^\dagger)^{11} \mu_3}{M_{S_2}^4 M_{\omega_3}^2}, \quad \epsilon_2^{RRL} = -\frac{1}{4}\epsilon_1^{RRL}. \quad (43)$$

The effective neutrino mass can be related to the first component of the neutrino mass matrix [78] and takes form as

$$|\langle m_{ee} \rangle| = \left| \sum_i U_{ei}^2 m_i \right| = |M_\nu^{11}| \simeq \frac{3\mu m_b}{16\pi^4 M_S^2} \tilde{I} \left(\frac{M_\omega^2}{M_S^2} \right) \left\{ m_s |y_{S(L)}^{21} y_{S(L)}^{31} z_\omega^{23}| + m_b |[y_{S(L)}^{31}]^2 z_\omega^{33}| \right\}. \quad (44)$$

The term related to m_s cannot be neglected because we have assumed that there is a hierarchy among the couplings z_ω^{ij} .

B. Numerical results

Before we give our numerical results, it is necessary to notice that the QCD corrections can modify the NMEs [79–84]. If we consider the leading order QCD corrections and the numerical values of the RGE μ -evolution matrix elements with the same chiral quark currents [80]

$$\hat{U}_{(12)}^{XX} = \begin{pmatrix} 2.39 & 0.02 \\ -3.83 & 0.35 \end{pmatrix}, \quad \hat{U}_{(3)}^{XX} = 0.70, \quad \hat{U}_{(45)}^{XX} = \begin{pmatrix} 0.35 & -0.96i \\ -0.06i & 2.39 \end{pmatrix}, \quad (45)$$

the NMEs need to be recomposited as

$$\mathcal{M}_1^{XX} \rightarrow \beta_1^{XX} = 2.39\mathcal{M}_1^{XX} - 3.83\mathcal{M}_2^{XX}, \quad (46)$$

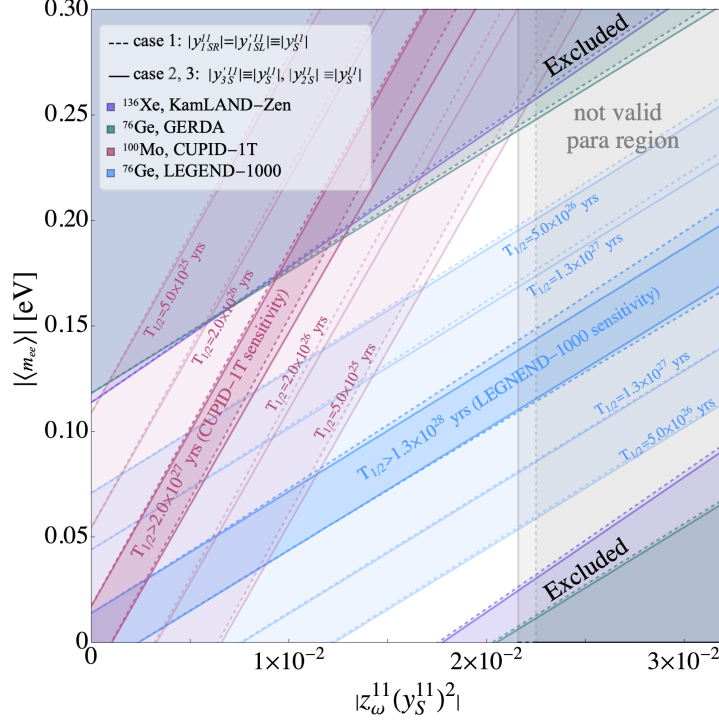


FIG. 4. The contour with the effective neutrino mass $|\langle m_{ee} \rangle|$ in the unit of eV and the couplings $|z_\omega^{11}(y_S^{11})^2|$. The lines show the experimental bound of $0\nu\beta\beta$ decay half-life in different cases and different isotopes. The upper and lower corner regions are excluded by KamLAND-Zen and GERDA experiments. The red and blue regions correspond to the experiments CUPID-1T and LEGEND-1000. The corresponding experiments are shown in the legends. The gray region is not valid in our numerical analysis. Here we take $\mu = M_S = 1.5$ TeV and $M_\omega = 8$ TeV. We assume that $|y_{1SR}^{11}| = |y_{1SL}^{11}|$ in case 1 and denote $|y_{1SR}^{11}|$, $|y_{1SL}^{11}|$, $|y_{3S}^{11}|$, and $|y_{2S}^{11}|$ as $|y_S^{11}|$.

$$\mathcal{M}_2^{XX} \rightarrow \beta_2^{XX} = 0.02\mathcal{M}_1^{XX} + 0.35\mathcal{M}_2^{XX}, \quad (47)$$

$$\mathcal{M}_3^{XX} \rightarrow \beta_3^{XX} = 0.70\mathcal{M}_3^{XX}, \quad (48)$$

$$\mathcal{M}_4^{XX} \rightarrow \beta_4^{XX} = 0.35\mathcal{M}_4^{XX} - 0.06i\mathcal{M}_5^{XX}, \quad (49)$$

$$\mathcal{M}_5^{XX} \rightarrow \beta_5^{XX} = -0.96i\mathcal{M}_4^{XX} + 2.39\mathcal{M}_5^{XX}. \quad (50)$$

The inverse half-life $[T_{1/2}^{0\nu\beta\beta}]^{-1}(G_{jk}, \epsilon_i, \mathcal{M}_i)$ have to be replaced with $[T_{1/2}^{0\nu\beta\beta}]^{-1}(G_{jk}, \epsilon_i, \beta_i)$. After considering the experimental values and substituting the numerical values of the PSFs and the NMEs shown in Table III and IV, one can get the limits on the couplings.

We show the contour with the effective neutrino mass $|\langle m_{ee} \rangle|$ in the unit of eV and the couplings $|z_\omega^{11}(y_S^{11})^2|$ in Fig. 4 and Fig. 5. The purple and green regions (upper and lower corners) are excluded by the $0\nu\beta\beta$ decay experiments KamLAND-Zen [9] and GERDA [10]. The red and blue regions correspond to the survival areas for the experiments CUPID-1T [11] and LEGEND-1000 [12] if we assume that no signals are found and set the half-lifetime to $T_{1/2} > 5.0 \times 10^{25}$ yrs (CUPID) and 5.0×10^{26} yrs (LEGEND), whereas the inner darker areas relate to the sensitivities. We show all the three cases in Fig. 4, with the assumption $|y_{1SL}^{11}| = |y_{1SR}^{11}|$ for case 1. Under this assumption, the term that contains $\epsilon_{1,2}^{RRL}$ and ϵ_ν dominants in the inverse half-life expression. Due

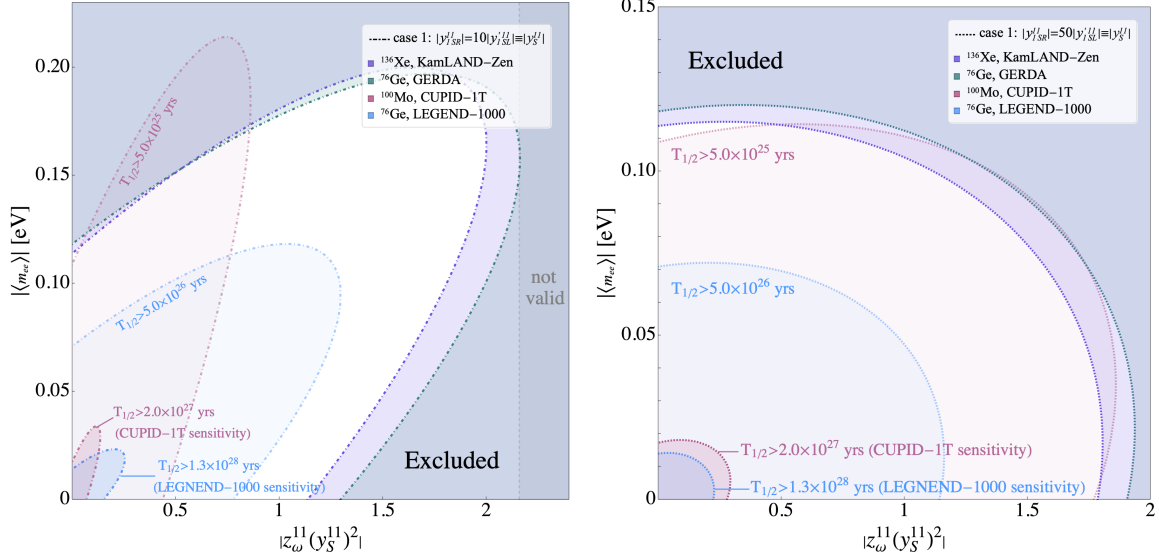


FIG. 5. The contour with the effective neutrino mass $|\langle m_{ee} \rangle|$ in the unit of eV and the couplings $|z_\omega^{11}(y_S^{11})^2|$ in case 1. Here we take $\mu = M_S = 1.5$ TeV and $M_\omega = 8$ TeV. We assume that $|y_{1SR}^{11}| = 10|y_{1SL}^{11}|$ (left) and $|y_{1SR}^{11}| = 50|y_{1SL}^{11}|$ (right), where $|y_{1SR}^{11}|$ is denoted as $|y_S^{11}|$.

to the cancellation between the standard light neutrino exchange contribution and the new physics contribution, the $0\nu\beta\beta$ decay could be hidden when the relations are linear or almost linear,

$$(y_S^{*11})^2 z_\omega^{11} \simeq 300 \times \frac{\mathcal{M}_\nu}{\beta_1 - \beta_2/4} \frac{\langle m_{ee} \rangle}{\text{eV}} \times \left(\frac{1.5 \text{ TeV}}{\mu} \right) \left(\frac{M_S}{1.5 \text{ TeV}} \right)^4 \left(\frac{M_\omega}{8 \text{ TeV}} \right)^2, \quad (51)$$

where the specific value of $\mathcal{M}_\nu/(\beta_1 - \beta_2/4)$ varies from isotope to isotope. For the current experiments, the relation can be realized successfully due to the similar ratio value of $\mathcal{M}_\nu/(\beta_1 - \beta_2/4)$ in ^{76}Ge and ^{136}Xe isotopes. Things will be different and intriguing when the next-generation experiments with ^{100}Mo isotope, e.g. AMoRE-II [85] and CUPID-1T, push the half-life to be order of 10^{26} yrs. The slope of the band with ^{100}Mo is different from ^{76}Ge or ^{136}Xe , leading to the overlap of survival areas being narrowed. With the high sensitivity of the future CUPID-1T and LEGEND-1000 experiments, the survival band can be examined comprehensively. If there is no signal of $0\nu\beta\beta$ decays, the survival region will be reduced to the overlap area. On the other hand, if we see the signals in one experiment, the corresponding contour lines will be suitable. The other experiment can help us search for the appropriate region of the lines.

We show the contour of case 1 with assumption $|y_{1SL}^{11}| \ll |y_{1SR}^{11}| \equiv |y_S^{11}|$ in Fig. 5. This assumption is natural as the allowed regions have ten times difference, and the influence on the neutrino mass is negligible. The survival region is elliptical instead. The left panel refers to $|y_{1SR}^{11}| = 10|y_{1SL}^{11}|$. One can find that the constraint on the effective Majorana neutrino mass can be larger than the one with only standard neutrino exchange considered $|\langle m_{ee} \rangle| \lesssim 0.2$ eV. The experiment with ^{100}Mo isotopes can help to reduce the survival area which is similar to what we discussed before. The right panel refers to $|y_{1SR}^{11}| = 50|y_{1SL}^{11}|$ and the effect of the combined analysis with different experiments is not apparent. The bound on the couplings given by experiments

KamLAND-Zen and GERDA are

$$|z_\omega^{11}(y_S^{11})^2| < 1.8 \times \left(\frac{1.5 \text{ TeV}}{\mu} \right) \left(\frac{M_S}{1.5 \text{ TeV}} \right)^4 \left(\frac{M_\omega}{8 \text{ TeV}} \right)^2. \quad (52)$$

The limits will be more stringent in next generation $0\nu\beta\beta$ decay experiments, which have the potential to restrict $|z_\omega^{11}(y_S^{11})^2|$ at $\mathcal{O}(10^{-1})$ scale.

IV. SUMMARY

In this paper, we have discussed the neutrinoless double beta decay in the colored Zee-Babu model. We study all three cases for the colored Zee-Babu model with a leptoquark and a diquark. The tiny neutrino masses are generated at two-loop level, and neutrinoless double beta decay gets additional contribution from the leptoquarks. We set some texture zeros for the Yukawa coupling matrices to evade constraints from various lepton flavor violation processes. We obtain the allowed regions of parameters after considering the constraints given by tree-level flavor violation processes and charged lepton anomalous magnetic moment.

We have discussed the short-range and standard neutrino exchange mechanisms of neutrinoless double beta decay for each case. The short-range contribution can be realized at tree-level. The general formula of the short-range contributions via the effective field theory approach is briefly reviewed. We adopt the values of nuclear matrix elements calculated with the microscopic interacting boson model and consider the leading order QCD running correction. We give numerical analysis for the three cases with the current experimental results and sensitivities of next-generation experiments. We find that the neutrinoless double beta decay can be hidden with a linear relation in all the cases under certain conditions. The relation can be examined by future $0\nu\beta\beta$ decay experiments. The complementary analysis of the different isotope experiments can help reduce the overlap area of the survival region.

Acknowledgements. This work is supported in part by the National Science Foundation of China (12175082, 11775093).

-
- [1] T. P. Cheng and L.-F. Li, Phys. Rev. D **22**, 2860 (1980).
 - [2] S. T. Petcov and S. T. Toshev, Phys. Lett. B **143**, 175 (1984).
 - [3] A. Zee, Nucl. Phys. B **264**, 99 (1986).
 - [4] K. S. Babu, Phys. Lett. B **203**, 132 (1988).
 - [5] K. S. Babu and J. Julio, Nucl. Phys. B **841**, 130 (2010), 1006.1092.
 - [6] P. W. Angel, Y. Cai, N. L. Rodd, M. A. Schmidt, and R. R. Volkas, JHEP **10**, 118 (2013), [Erratum: JHEP **11**, 092 (2014)], 1308.0463.
 - [7] D. Aristizabal Sierra, A. Degee, L. Dorame, and M. Hirsch, JHEP **03**, 040 (2015), 1411.7038.
 - [8] Q.-H. Cao, S.-L. Chen, E. Ma, B. Yan, and D.-M. Zhang, Phys. Lett. B **779**, 430 (2018), 1707.05896.
 - [9] A. Gando et al. (KamLAND-Zen), Phys. Rev. Lett. **117**, 082503 (2016), [Addendum: Phys.Rev.Lett. **117**, 109903 (2016)], 1605.02889.
 - [10] M. Agostini et al. (GERDA), Phys. Rev. Lett. **125**, 252502 (2020), 2009.06079.

- [11] A. Armatol et al. (CUPID) (2022), 2203.08386.
- [12] N. Abgrall et al. (LEGEND) (2021), 2107.11462.
- [13] G. Prezeau, M. Ramsey-Musolf, and P. Vogel, Phys. Rev. D **68**, 034016 (2003), hep-ph/0303205.
- [14] F. del Aguila, A. Aparici, S. Bhattacharya, A. Santamaria, and J. Wudka, JHEP **06**, 146 (2012), 1204.5986.
- [15] V. Cirigliano, W. Dekens, J. de Vries, M. L. Graesser, and E. Mereghetti, JHEP **12**, 082 (2017), 1708.09390.
- [16] F. F. Deppisch, L. Graf, J. Harz, and W.-C. Huang, Phys. Rev. D **98**, 055029 (2018), 1711.10432.
- [17] V. Cirigliano, W. Dekens, J. de Vries, M. L. Graesser, and E. Mereghetti, JHEP **12**, 097 (2018), 1806.02780.
- [18] L. Gráf, M. Lindner, and O. Scholer (2022), 2204.10845.
- [19] H. Pas, M. Hirsch, S. G. Kovalenko, and H. V. Klapdor-Kleingrothaus, Prog. Part. Nucl. Phys. **40**, 283 (1998), hep-ph/9712361.
- [20] H. Pas, M. Hirsch, H. V. Klapdor-Kleingrothaus, and S. G. Kovalenko, Phys. Lett. B **453**, 194 (1999).
- [21] J. C. Helo, M. Hirsch, and T. Ota, JHEP **06**, 006 (2016), 1602.03362.
- [22] J. Kotila, J. Ferretti, and F. Iachello (2021), 2110.09141.
- [23] H. Pas, M. Hirsch, H. V. Klapdor-Kleingrothaus, and S. G. Kovalenko, Phys. Lett. B **498**, 35 (2001), hep-ph/0008182.
- [24] L. Graf, F. F. Deppisch, F. Iachello, and J. Kotila, Phys. Rev. D **98**, 095023 (2018), 1806.06058.
- [25] F. Bonnet, M. Hirsch, T. Ota, and W. Winter, JHEP **03**, 055 (2013), [Erratum: JHEP 04, 090 (2014)], 1212.3045.
- [26] P.-T. Chen, G.-J. Ding, and C.-Y. Yao, JHEP **12**, 169 (2021), 2110.15347.
- [27] J. C. Helo, M. Hirsch, H. Päs, and S. G. Kovalenko, Phys. Rev. D **88**, 073011 (2013), 1307.4849.
- [28] F. F. Deppisch, L. Graf, F. Iachello, and J. Kotila, Phys. Rev. D **102**, 095016 (2020), 2009.10119.
- [29] M. Kohda, H. Sugiyama, and K. Tsumura, Phys. Lett. B **718**, 1436 (2013), 1210.5622.
- [30] T. Nomura and H. Okada, Phys. Rev. D **94**, 075021 (2016), 1607.04952.
- [31] W.-F. Chang, S.-C. Liou, C.-F. Wong, and F. Xu, JHEP **10**, 106 (2016), 1608.05511.
- [32] S.-Y. Guo, Z.-L. Han, B. Li, Y. Liao, and X.-D. Ma, Nucl. Phys. B **928**, 435 (2018), 1707.00522.
- [33] R. Ding, Z.-L. Han, L. Huang, and Y. Liao, Chin. Phys. C **42**, 103101 (2018), 1802.05248.
- [34] A. Datta, D. Sachdeva, and J. Waite, Phys. Rev. D **100**, 055015 (2019), 1905.04046.
- [35] S. Saad, Phys. Rev. D **102**, 015019 (2020), 2005.04352.
- [36] K. S. Babu, P. S. B. Dev, S. Jana, and A. Thapa, JHEP **03**, 179 (2021), 2009.01771.
- [37] M. Hirsch, H. V. Klapdor-Kleingrothaus, and S. G. Kovalenko, Phys. Lett. B **378**, 17 (1996), hep-ph/9602305.
- [38] M. Hirsch, H. V. Klapdor-Kleingrothaus, and S. G. Kovalenko, Phys. Rev. D **54**, R4207 (1996), hep-ph/9603213.
- [39] A. J. Davies and X.-G. He, Phys. Rev. D **43**, 225 (1991).
- [40] I. Doršner, S. Fajfer, A. Greljo, J. F. Kamenik, and N. Košnik, Phys. Rept. **641**, 1 (2016), 1603.04993.
- [41] A. M. Sirunyan et al. (CMS), Phys. Rev. D **99**, 052002 (2019), 1811.01197.
- [42] G. Aad et al. (ATLAS), JHEP **10**, 112 (2020), 2006.05872.
- [43] M. Aaboud et al. (ATLAS), Eur. Phys. J. C **79**, 733 (2019), 1902.00377.
- [44] A. M. Sirunyan et al. (CMS), Phys. Rev. D **99**, 032014 (2019), 1808.05082.
- [45] A. M. Sirunyan et al. (CMS), Eur. Phys. J. C **78**, 707 (2018), 1803.02864.
- [46] S. Chatrchyan et al. (CMS), JHEP **12**, 055 (2012), 1210.5627.
- [47] A. M. Sirunyan et al. (CMS), JHEP **05**, 033 (2020), 1911.03947.
- [48] K. S. Babu and C. Macesanu, Phys. Rev. D **67**, 073010 (2003), hep-ph/0212058.

- [49] K. Abe et al. (Super-Kamiokande), Phys. Rev. D **103**, 012008 (2021), 2012.02607.
- [50] L. N. Chang and N. P. Chang, Phys. Lett. B **92**, 103 (1980).
- [51] T.-K. Kuo and S. T. Love, Phys. Rev. Lett. **45**, 93 (1980).
- [52] S. Rao and R. Shrock, Phys. Lett. B **116**, 238 (1982).
- [53] S. Rao and R. E. Shrock, Nucl. Phys. B **232**, 143 (1984).
- [54] W. E. Caswell, J. Milutinovic, and G. Senjanovic, Phys. Lett. B **122**, 373 (1983).
- [55] M. I. Buchoff and M. Wagman, Phys. Rev. D **93**, 016005 (2016), [Erratum: Phys.Rev.D 98, 079901 (2018)], 1506.00647.
- [56] E. Rinaldi, S. Syritsyn, M. L. Wagman, M. I. Buchoff, C. Schroeder, and J. Wasem, Phys. Rev. D **99**, 074510 (2019), 1901.07519.
- [57] F. Oosterhof, B. Long, J. de Vries, R. G. E. Timmermans, and U. van Kolck, Phys. Rev. Lett. **122**, 172501 (2019), 1902.05342.
- [58] K. Fridell, J. Harz, and C. Hati, JHEP **11**, 185 (2021), 2105.06487.
- [59] A. Takenaka et al. (Super-Kamiokande), Phys. Rev. D **102**, 112011 (2020), 2010.16098.
- [60] Y. Aoki, T. Izubuchi, E. Shintani, and A. Soni, Phys. Rev. D **96**, 014506 (2017), 1705.01338.
- [61] J.-S. Yoo, Y. Aoki, P. Boyle, T. Izubuchi, A. Soni, and S. Syritsyn, Phys. Rev. D **105**, 074501 (2022), 2111.01608.
- [62] F. Capozzi, E. Lisi, A. Marrone, and A. Palazzo, Prog. Part. Nucl. Phys. **102**, 48 (2018), 1804.09678.
- [63] I. Esteban, M. C. Gonzalez-Garcia, M. Maltoni, T. Schwetz, and A. Zhou, JHEP **09**, 178 (2020), 2007.14792.
- [64] P. F. de Salas, D. V. Forero, C. A. Ternes, M. Tortola, and J. W. F. Valle, Phys. Lett. B **782**, 633 (2018), 1708.01186.
- [65] P. F. de Salas, D. V. Forero, S. Gariazzo, P. Martínez-Miravé, O. Mena, C. A. Ternes, M. Tórtola, and J. W. F. Valle, JHEP **02**, 071 (2021), 2006.11237.
- [66] S. Davidson, D. C. Bailey, and B. A. Campbell, Z. Phys. C **61**, 613 (1994), hep-ph/9309310.
- [67] M. Leurer, Phys. Rev. D **49**, 333 (1994), hep-ph/9309266.
- [68] M. Leurer, Phys. Rev. D **50**, 536 (1994), hep-ph/9312341.
- [69] M. Carpentier and S. Davidson, Eur. Phys. J. C **70**, 1071 (2010), 1008.0280.
- [70] M. Bona et al. (UTfit), JHEP **03**, 049 (2008), 0707.0636.
- [71] B. Abi et al. (Muon g-2), Phys. Rev. Lett. **126**, 141801 (2021), 2104.03281.
- [72] F. S. Queiroz and W. Shepherd, Phys. Rev. D **89**, 095024 (2014), 1403.2309.
- [73] J. Kotila and F. Iachello, Phys. Rev. C **85**, 034316 (2012), 1209.5722.
- [74] O. Azzolini et al. (CUPID-0), Phys. Rev. Lett. **120**, 232502 (2018), 1802.07791.
- [75] E. Armengaud et al. (CUPID), Phys. Rev. Lett. **126**, 181802 (2021), 2011.13243.
- [76] C. Arnaboldi et al., Phys. Lett. B **557**, 167 (2003), hep-ex/0211071.
- [77] D. Q. Adams et al. (CUORE) (2021), 2104.06906.
- [78] J. C. Helo, M. Hirsch, T. Ota, and F. A. Pereira dos Santos, JHEP **05**, 092 (2015), 1502.05188.
- [79] N. Mahajan, Phys. Rev. Lett. **112**, 031804 (2014), 1310.1064.
- [80] M. González, M. Hirsch, and S. G. Kovalenko, Phys. Rev. D **93**, 013017 (2016), [Erratum: Phys.Rev.D 97, 099907 (2018)], 1511.03945.
- [81] C. Arbeláez, M. González, M. Hirsch, and S. Kovalenko, Phys. Rev. D **94**, 096014 (2016), [Erratum: Phys.Rev.D 97, 099904 (2018)], 1610.04096.
- [82] C. Arbeláez, M. González, S. Kovalenko, and M. Hirsch, Phys. Rev. D **96**, 015010 (2017), 1611.06095.
- [83] M. González, M. Hirsch, and S. Kovalenko, Phys. Rev. D **97**, 115005 (2018), 1711.08311.
- [84] C. Ayala, G. Cvetič, and L. Gonzalez, Phys. Rev. D **101**, 094003 (2020), 2001.04000.
- [85] M. H. Lee (AMoRE), JINST **15**, C08010 (2020), 2005.05567.